Figures and figure supplements

The differentiation and integration of the hippocampal dorsoventral axis are controlled by two nuclear receptor genes

Xiong Yang and Rong Wan *et al.*

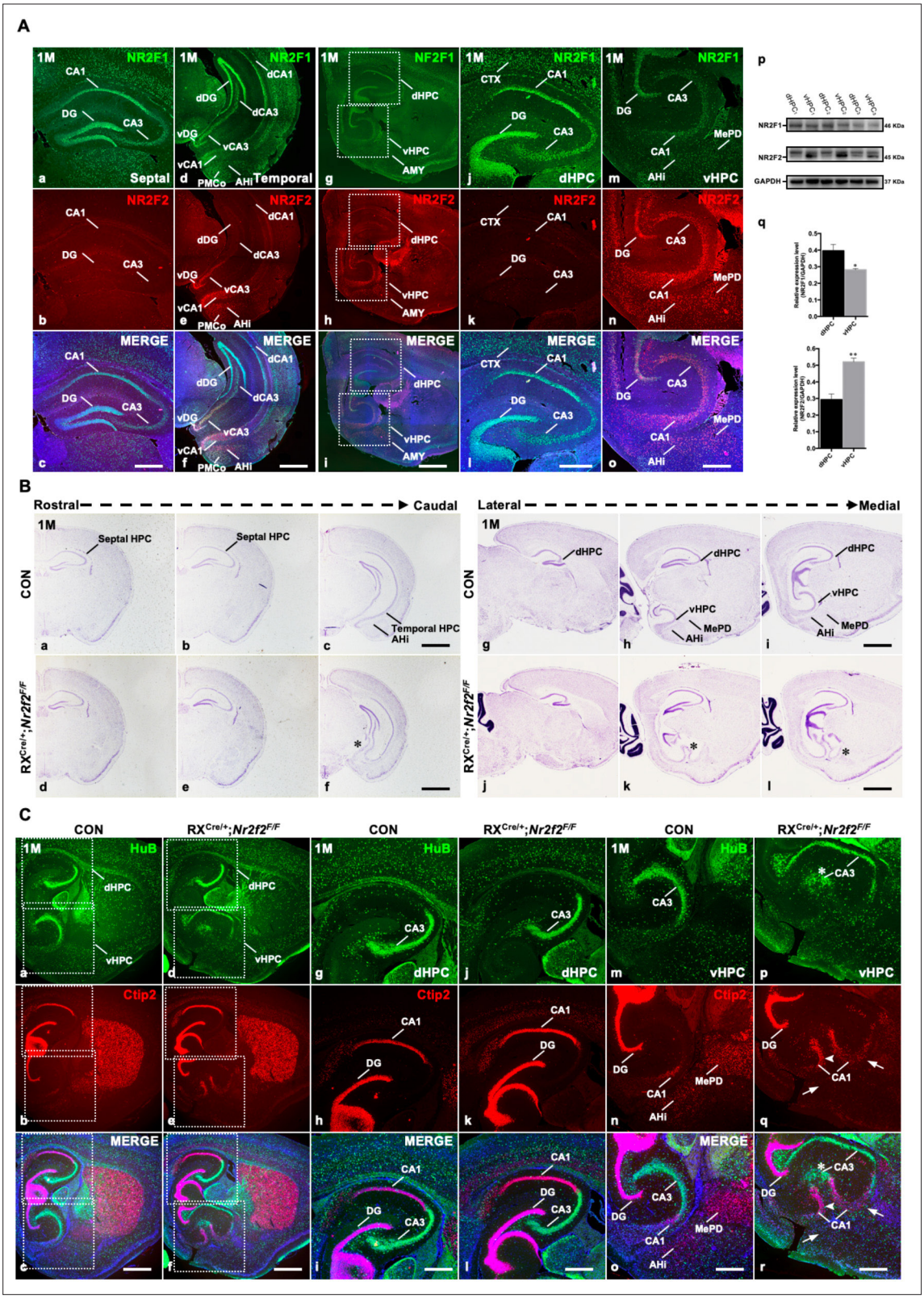

Figure 1. Duplicated CA1 and CA3 domains are generated in the ventral hippocampus of RX$^{Cre/+}$; *Nr2f2*$^{F/F}$ mutant mice. (**A**) The expression of NR2F1 (**a, d, g, j, m**) and NR2F2 (**b, e, h, k, n**) in coronal sections (**a–f**) and sagittal sections (**g–o**) of the hippocampus at postnatal month 1 (1M); representative western blots and quantitative densitometry data for the expression of NR2F1 and NR2F2 in the dorsal and ventral hippocampus at 1M (**p–q**). Data are presented as mean ± SEM. *Student's t test* was used in q, **P*<0.05, ***P*<0.01; n represents separate experiments, n=3. (**B**) In coronal sections along the

Figure 1 continued on next page

Figure 1 continued

rostrocaudal axis (**a–f**) and sagittal sections along the lateral-medial axis (**g–l**) of the hippocampus in mutant mice, compared with that in control mice (**a–c, g–i**), the ectopic CA-like structure, indicated by the star, was observed in the ventral region in *Nr2f2* gene mutant ($RX^{Cre/+}$; $Nr2f2^{F/F}$) mice at 1M (**d–f, j–l**). (**C**) The expression of HuB and Ctip2 in the corresponding inserted area in (**a–f**) under a high-magnification objective lens at 1M (**g–r**); compared with those of control mice (**a–c, g–i, m–o**), the duplicated HuB-positive CA3 domain, indicated by the star, and Ctip2-positive domains, indicated by the arrowhead, were specifically observed in the ventral hippocampus (**d–f, p–r**) but not in the dorsal hippocampus (**d–f, j–l**) of *Nr2f2* mutant mice at 1M; Ctip2-positive AHi and MePD amygdaloid nuclei were barely observed in the *Nr2f2* mutant mice, indicated by the arrows, instead of the ectopic CA domains at the prospective amygdaloid regions (**e–f, q–r**). AHi, amygdalohippocampal area; AMY, amygdala nuclei; CTX, cortex; dCA1, dorsal CA1; dCA3, dorsal CA3; dDG, dorsal dentate gyrus; dHPC, dorsal hippocampus; MePD, posterodorsal part of the medial amygdaloid nucleus; PMCo, posteromedial cortical amygdaloid nucleus; vCA1, ventral CA1; vCA3, ventral CA3; vDG, ventral dentate gyrus; vHPC, ventral hippocampus. Scale bars, (**Aa–c, Ad–f, Aj–o, Cg–r**), 100 μm; (**Ag–i, Ba–l, Ca–f**), 200 μm.

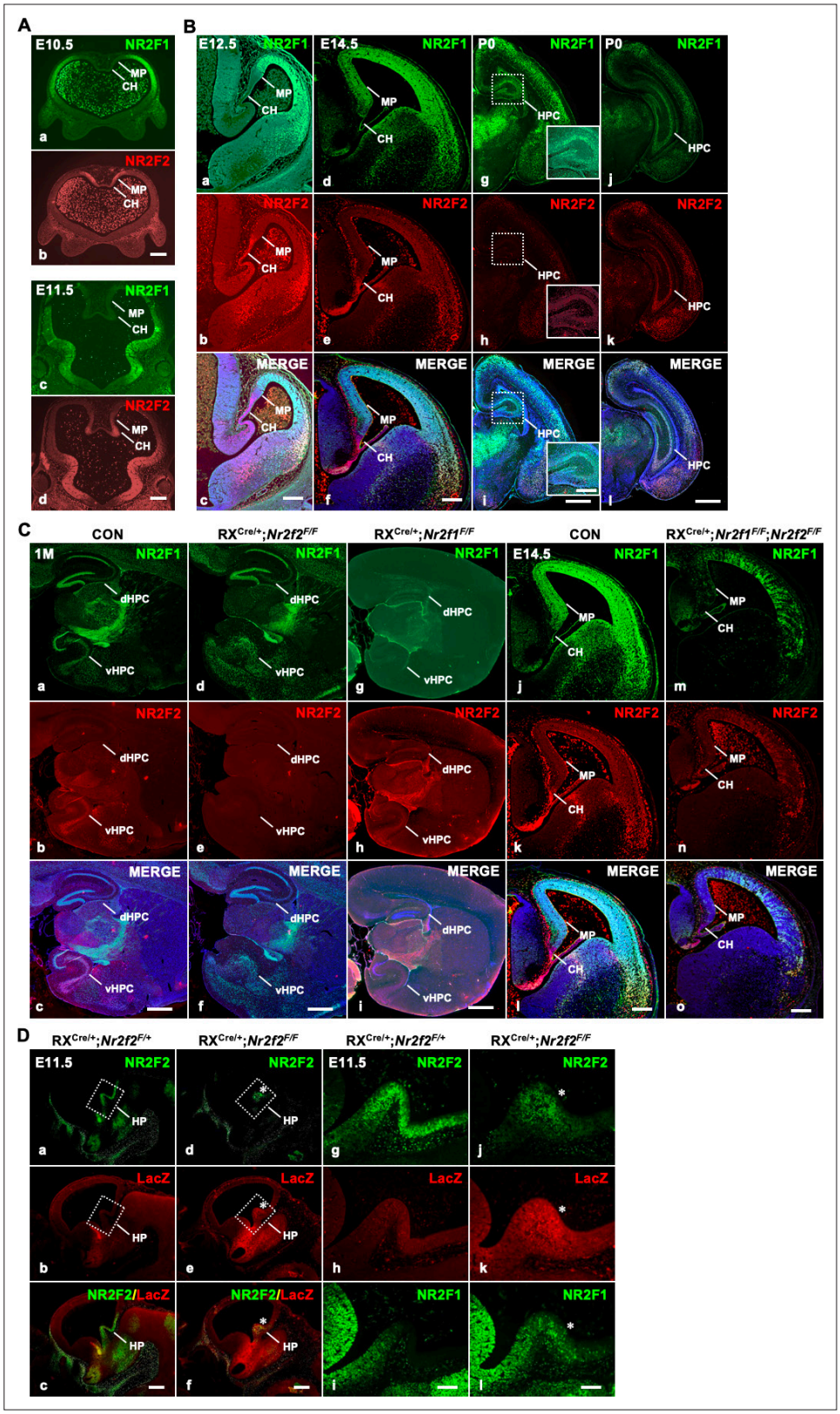

Figure 1—figure supplement 1. The expression of *Nr2f* genes in the early developing hippocampus and different conditional knock mouse models. (**A**) The expression of *Nr2f1* and *Nr2f2* genes in the forebrain at E10.5 (**a, b**) and E11.5 (**c, d**). (**B**) The expression of *Nr2f1* and *Nr2f2* genes in the developing hippocampus at E12.5 (**a–c**), E14.5 (**d–f**), and P0 (**g–l**). (**C**) Compared with that of control mice (**a–c**), *Nr2f2* is efficiently deleted by RXCre recombinase

Figure 1—figure supplement 1 continued on next page

Figure 1—figure supplement 1 continued

in the hippocampus of *Nr2f2* mutant mice at 1M (**d–f**); *Nr2f1* is clearly deleted by RXCre recombinase in the hippocampus of *Nr2f1* mutant mice at 1M (**g–i**). Compared with that of control mice (**j–l**), NR2F1 and NR2F2 were efficiently deleted by RXCre recombinase at the hippocampal primordium, including the MP and CH, in *Nr2f1/2* double-mutant mice at E14.5 (**m–o**). (**D**) Compared with that of the control mice (**a–c, g–h**), the expression of *Nr2f2* was significantly decreased in the hippocampal primordium of the homozygous mutant mice at E11.5; meanwhile, the LacZ signals obviously increased in the *Nr2f2* homozygous mutant mice at E11.5 (**d–f, j–k**). Compared with that of the control mice (**i**), the expression of NR2F1 is activated in the caudal hippocampal primordium of the homozygous mutant mice at E11.5 (**l**). CH, cortical hem; dHPC, dorsal hippocampus; HP, hippocampal primordium; HPC, hippocampus; MP, medial pallium; vHPC, ventral hippocampus. Scale bars, (**Aa–d, Ba–f, Bg-i (insets), Cj–o**), 200 μm; (**Bg–l, Ca–i, Dg–l**), 100 μm; (**Da–f**), 250 μm.

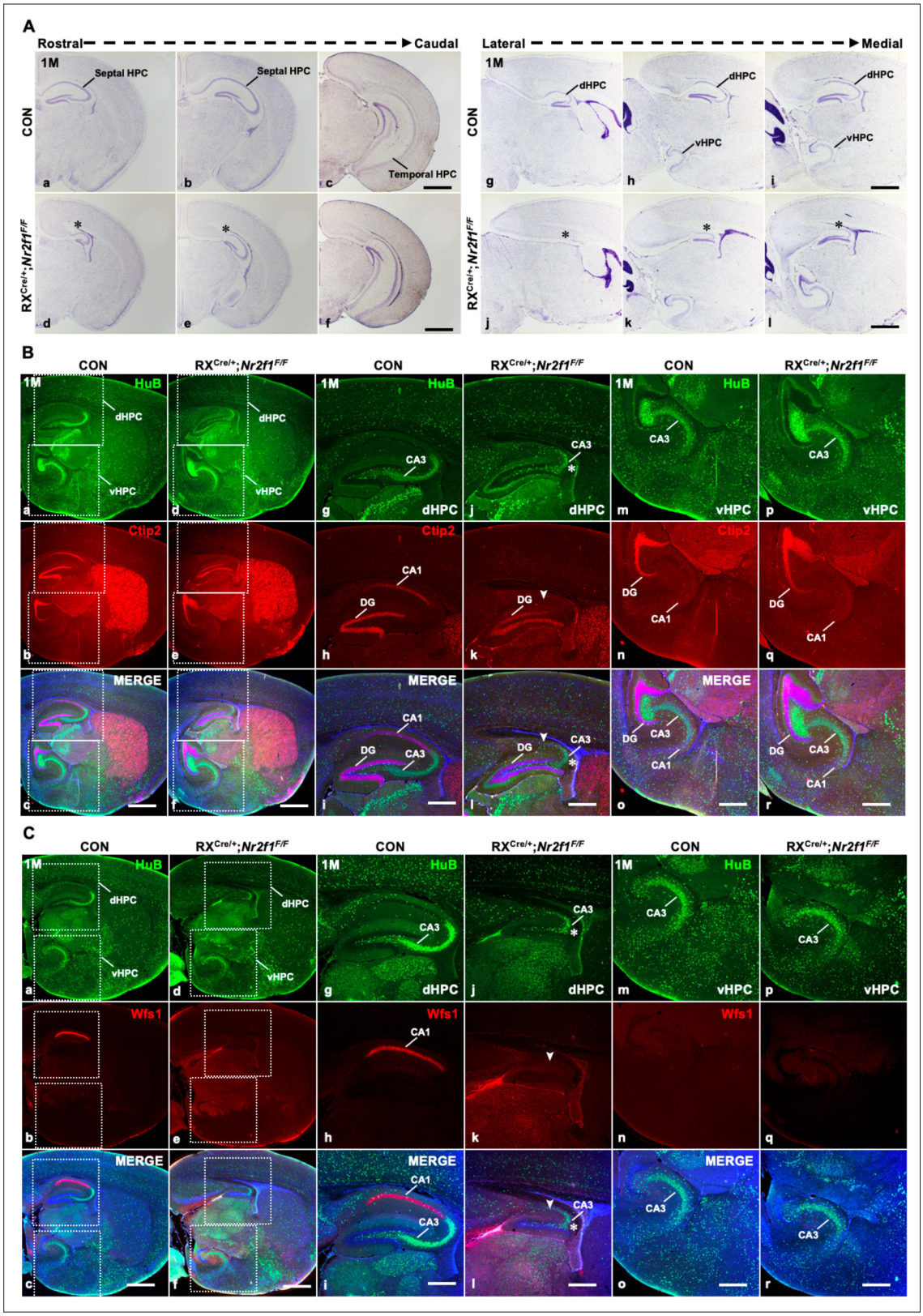

Figure 2. The specification and differentiation of the dorsal CA1 lineage failed with the dysplastic dorsal hippocampus in RX$^{Cre/+}$; *Nr2f1*$^{F/F}$ mutant mice. (**A**) In coronal sections along the rostrocaudal axis (**a–f**) and sagittal sections along the lateral–medial axis (**g–l**) of the hippocampus, compared with that of control mice (**a–c, g–i**), the dorsal hippocampus was shrunken, indicated by the star, in *Nr2f1* gene mutant (RX$^{Cre/+}$; *Nr2f1*$^{F/F}$) mice at 1M (**d–f, j–l**). (**B**) The expression of HuB and Ctip2 in the corresponding inserted area in (**a–f**) under a high-magnification objective lens at 1M (**g–r**); compared

Figure 2 continued on next page

Figure 2 continued

with that of control mice (**a–c, g–i, m–o**), the HuB-positive CA3 domain was reduced in the dorsal hippocampus, especially the Ctip2-positive dorsal CA1, which was barely detected in *Nr2f1* mutant mice at 1M (**d–f, j–l**), while their expression in the ventral hippocampus was comparable between the controls and mutants (**d–f, p–r**). (**C**) The expression of HuB and Wfs1 in the corresponding inserted area in (**a–f**) under a high-magnification objective lens at 1M (**g–r**); the expression of HuB and the dCA1 marker Wfs1 in the control (**a–c, g–i, m–o**) and *Nr2f2* mutant mice (**d–f, j–l, p–r**) at 1M. Wfs1-positive dorsal CA1 could not be detected in *Nr2f1* mutant mice at 1M, as indicated by the arrowhead. dHPC, dorsal hippocampus; HPC, hippocampus; vHPC, ventral hippocampus. Scale bars, (**Aa–l, Ba–f, Ca–f**), 200 μm; (**Bg–r, Cg–r**), 100 μm.

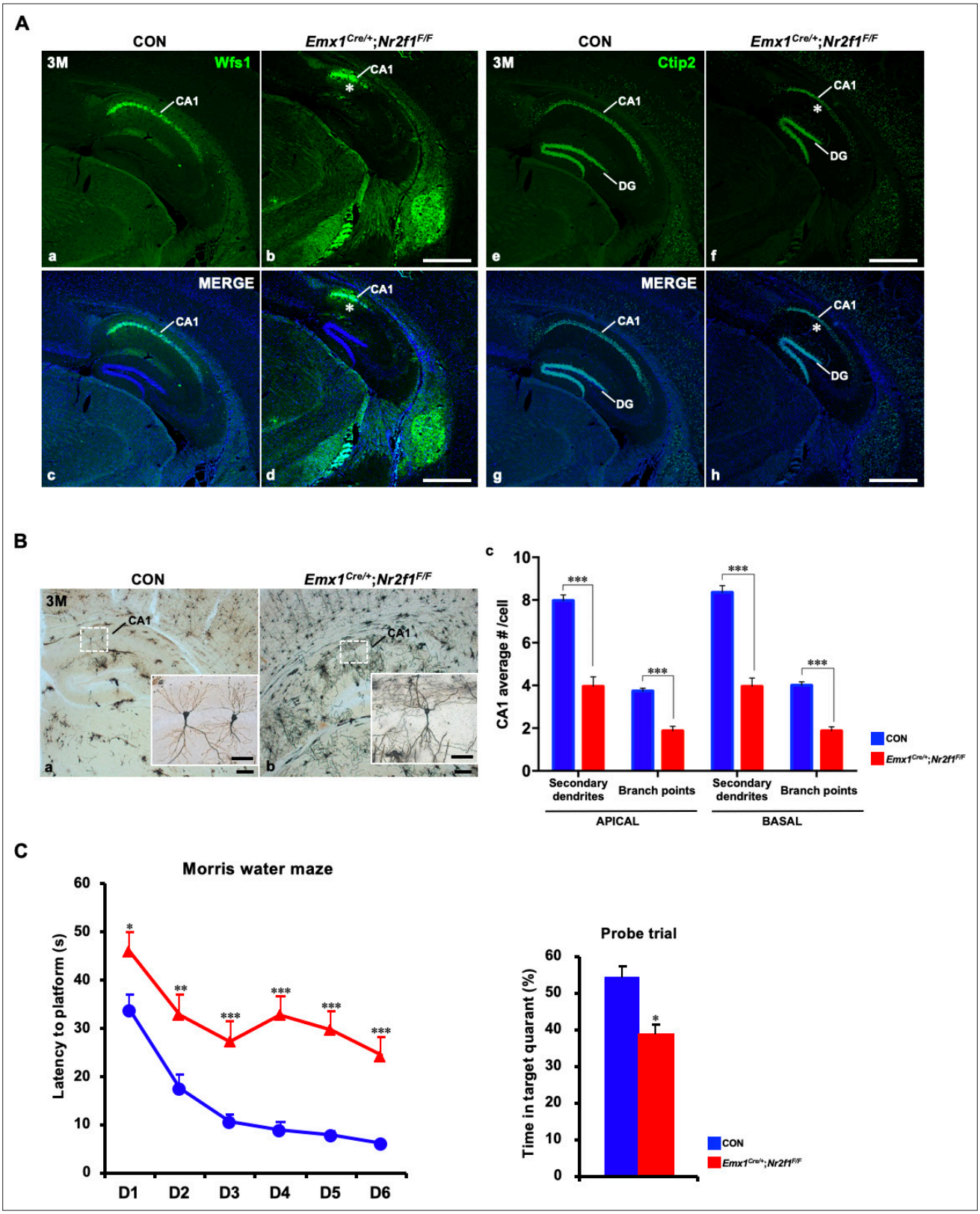

Figure 2—figure supplement 1. Defects in *Emx1*$^{Cre/+}$; *Nr2f1*$^{F/F}$ mutant mice. (**A**) Immunofluorescence staining data showed that compared with those of control mice (**a, c, e, g**), the proportions of either the Wfs1- or Ctip2-positive dorsal CA1 domain were reduced in *Emx1*$^{Cre/+}$; *Nr2f1*$^{F/F}$ mutant mice at 3M (**b, d, f, h**). (**B**) Golgi staining showed that compared with those of controls, the numbers of branch points and secondary dendrites of both apical and basal dendrites were significantly reduced in the dorsal hippocampal CA1 pyramidal neurons of *Emx1*$^{Cre/+}$; *Nr2f1*$^{F/F}$ mutant mice (**a–c**). Data

Figure 2—figure supplement 1 continued on next page

Figure 2—figure supplement 1 continued

are presented as mean ± SEM. *Student's t test* was used in c, ***$P<0.001$; n represents separate experiments, n=3. (**C**) The Morris water maze behavior test showed that compared with that of controls, spatial learning and memory were significantly damaged in *Emx1$^{Cre/+}$; Nr2f1$^{F/F}$* mutant mice. Data are presented as mean ± SEM. *Student's t test* was used in C, *p<0.05, **p<0.01, ***p<0.001; n represents animal number used in the experiments, n=12 (CON) and n=8 (*Emx1$^{Cre/+}$*; *Nr2f1$^{F/F}$*), 10 weeks or older adult male mice. Scale bars, (**Aa–h**), 100 μm; (**Ba–b**), 50 μm; (**Ba-b** (insets)), 200 μm.

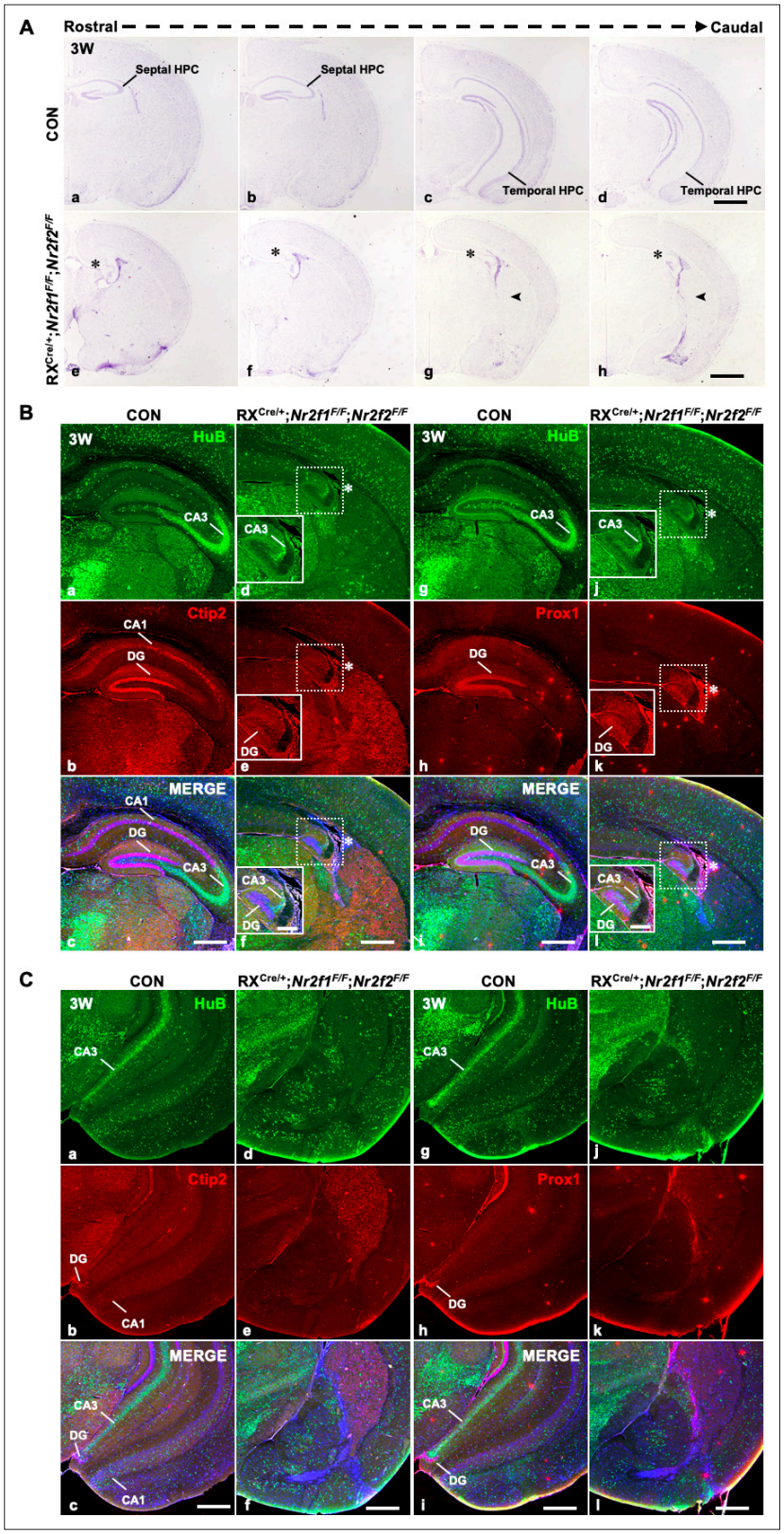

Figure 3. Defects in the hippocampus in RX$^{Cre/+}$; *Nr2f1*$^{F/F}$; *Nr2f2*$^{F/F}$ double-gene mutant mice. (**A**) In coronal sections along the rostrocaudal axis, compared with control mice (**a–d**), the hippocampus was atrophic in RX$^{Cre/+}$; *Nr2f1*$^{F/F}$; *Nr2f2*$^{F/F}$ double-mutant mice, indicated by the star, and an ectopic unknown nucleus was observed in the caudal plates, indicated by the arrowhead (**e–h**). (**B**) Compared with that of control mice (**a–c, g–i**), the expression of HuB,

Figure 3 continued on next page

Figure 3 continued

Ctip2, and Prox1 was decreased in the hippocampus of *Nr2f1/2* double-gene mutant mice at 3 weeks postnatal (3W) (**d–f, j–l**). (**C**) Compared with that of control mice (**a–c, g–i**), the expression of HuB could not be detected in the presumptive CA3 domain, and the expression of Ctip2 or Prox1 could not be detected in the presumptive DG domain of the prospective ventral hippocampus of $RX^{Cre/+}$; $Nr2f1^{F/F}$; $Nr2f2^{F/F}$ double-mutant mice. Scale bars, (**Aa–h**), 200 μm; (**Ba–l, Ca–l**), 100 μm; (**Bd-f** (insets), **Bj-l** (insets)), 400 μm.

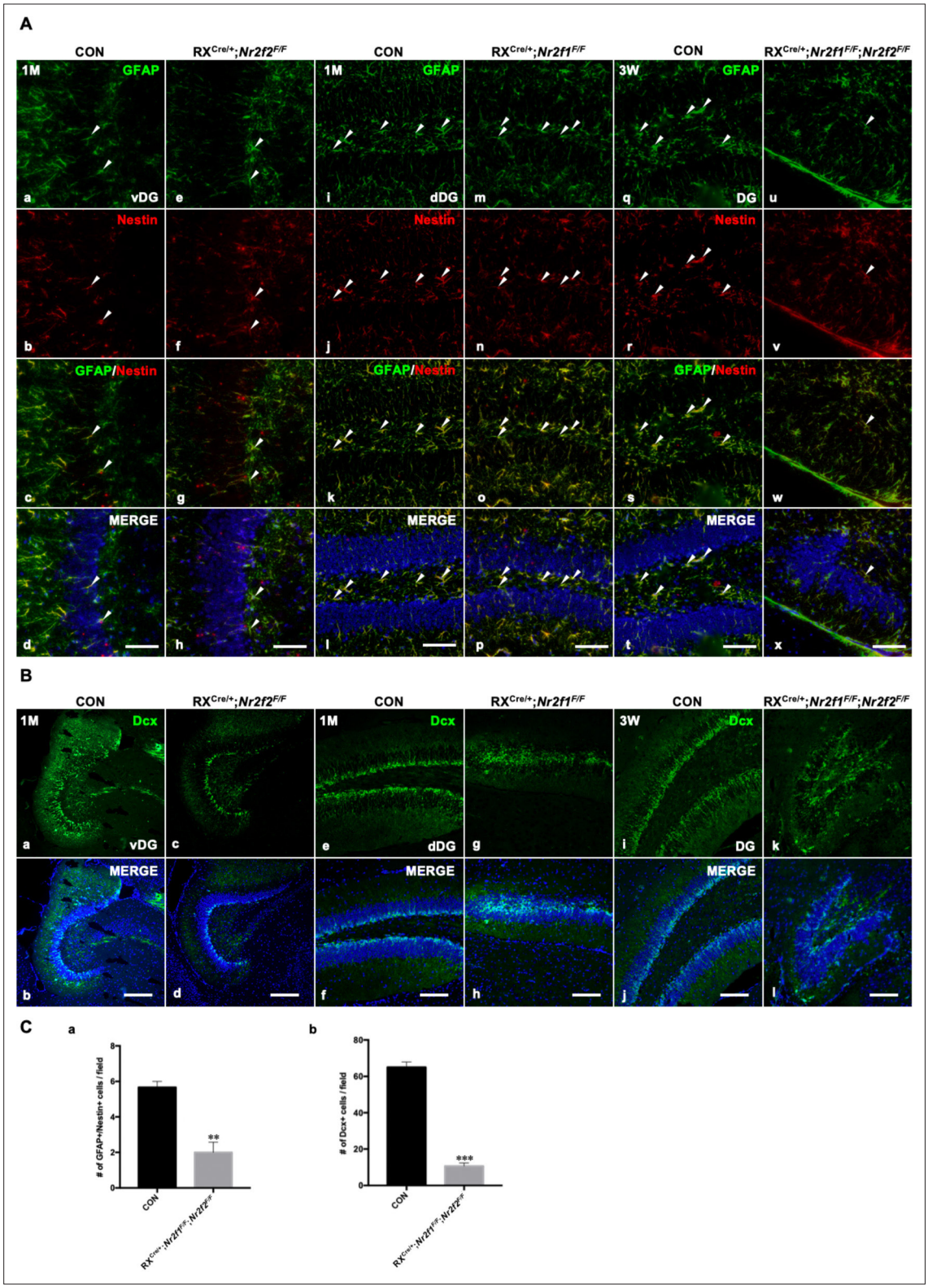

Figure 3—figure supplement 1. Adult neurogenesis was abnormal in the hippocampi of *Nr2f1/2* double-gene mutant mice. (**A**) The expression of GFAP and Nestin, markers of NSCs, in the SGZ of the vDG in control and *Nr2f2* mutant mice at 1M (**a–h**), in the SGZ of the dDG in control and *Nr2f1* mutant mice at 1M (**i–p**) and in the SGZ of the DG in control and *Nr2f1/2* double-gene mutant mice at 3W (**q–x**). (**B**) The expression of Dcx, a marker of newborn neurons, in the SGZ of the vDG in control and *Nr2f2* mutant mice at 1M (**a–d**), in the SGZ of the dDG in control and *Nr2f1* mutant mice at 1M (**e–h**) and in the SGZ of the DG in control and *Nr2f1/2* double-gene mutant mice at 3W (**i–l**). (**C**) Quantitative analysis of GFAP/Nestin-positive cells

Figure 3—figure supplement 1 continued on next page

Figure 3—figure supplement 1 continued

(**a**) and Dcx-positive cells (**b**) in the SGZ of the DG in control and *Nr2f1/2* double-gene mutant mice at 3W. The numbers of GFAP and Nestin double-positive NSCs and Dcx-positive newborn neurons were significantly reduced in double-mutant mice. Data are presented as mean ± SEM. *Student's t-test* was used in C, $^{**}p<0.01$, $^{***}p<0.001$; n represents separate experiments, n=3. DG, dentate gyrus; dDG, dorsal DG; NSC, neural stem cell; SGZ, subgranular zone; vDG, ventral DG. Scale bars, (**Aa–x**), 50 μm; (**Ba–l**), 100 μm.

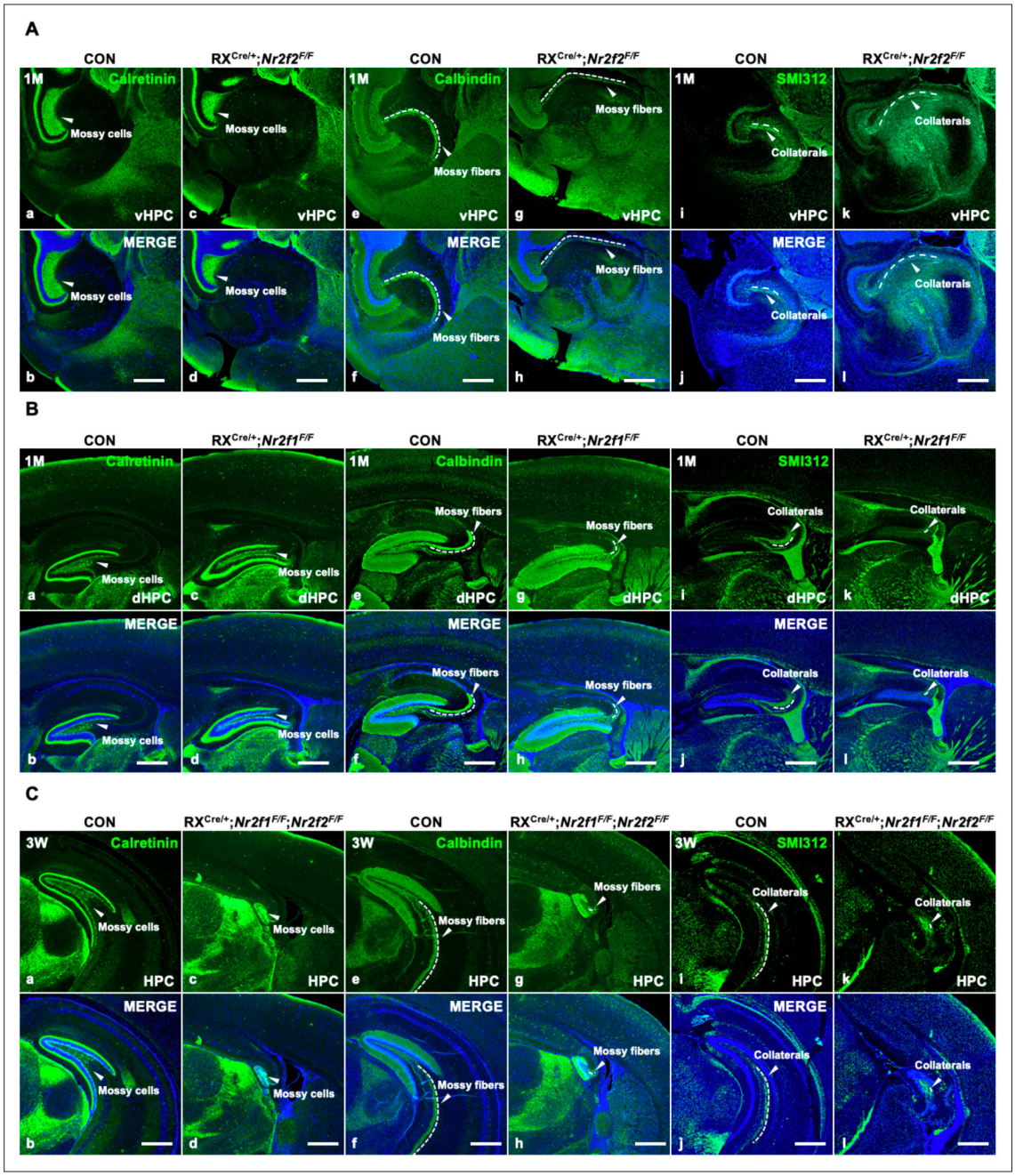

Figure 4. The impairment of hippocampal trisynaptic connectivity in *Nr2f2* single-gene, *Nr2f1* single-gene, and *Nr2f1/2* double-gene mutant mice. (**A**) The expression of Calretinin, Calbindin, and SMI312 in the ventral hippocampus of the control (**a, b, e, f, i, j**) and *Nr2f2* single-gene mutant mice (**c, d, g, h, k, l**). (**B**) The expression of Calretinin, Calbindin, and SMI312 in the dorsal hippocampus of the control (**a, b, e, f, i, j**) and *Nr2f1* single-gene mutant mice (**c, d, g, h, k, l**). (**C**) The expression of Calretinin, Calbindin, and SMI312 in the hippocampus of the control (**a, b, e, f, i, j**) and *Nr2f1/2* double-gene mutant mice (**c, d, g, h, k, l**). dHPC, dorsal hippocampus; HPC, hippocampus; vHPC, ventral hippocampus. Scale bars, (**Aa–l**, **Ba–l**, **Ca–l**), 100 μm.

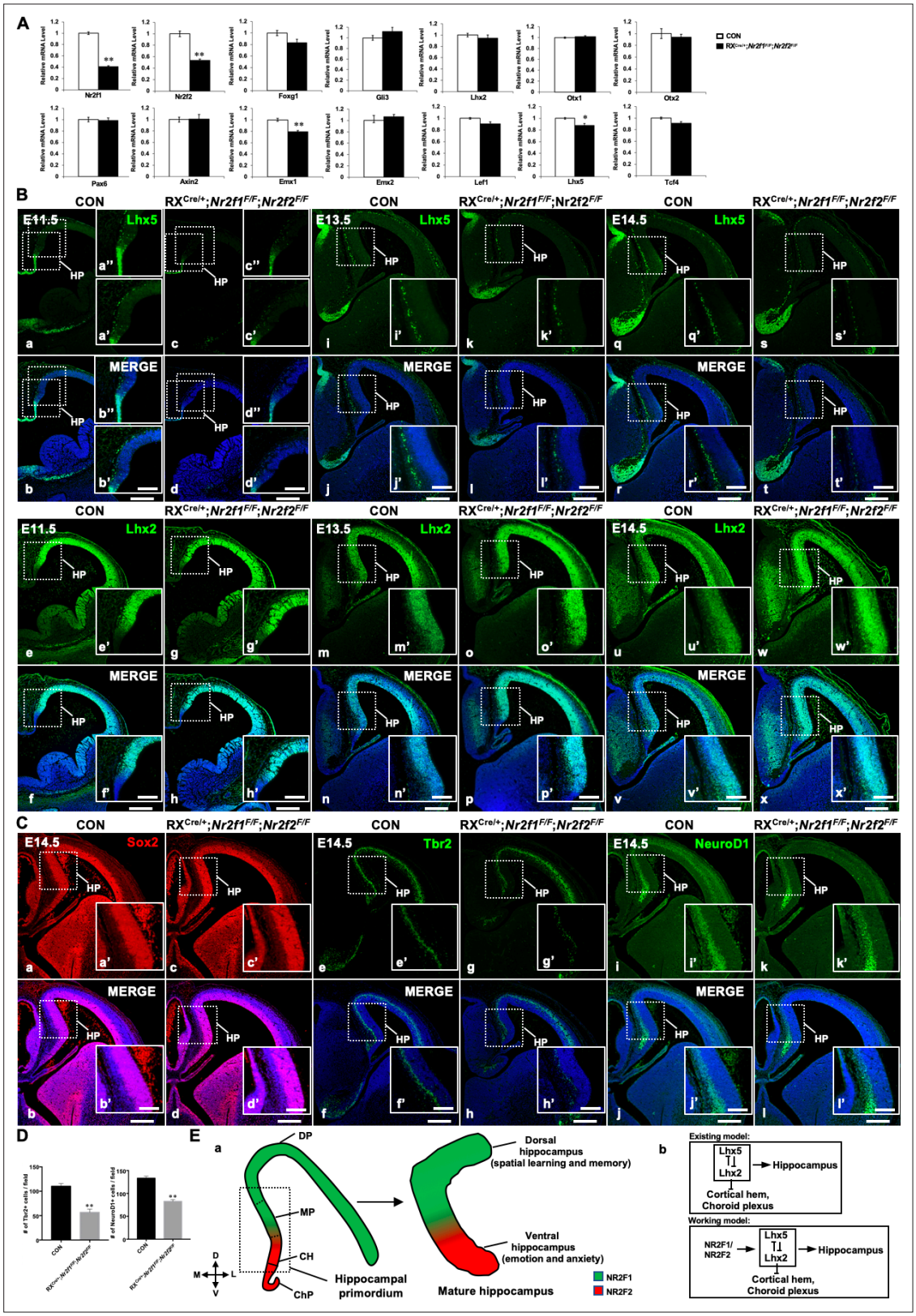

Figure 5. *Nr2f* genes regulate the expression of key genes associated with early hippocampal development. (**A**) The expression profiles of genes involved in hippocampal development in control and the double-mutant mice at E11.5. Data are presented as mean ± SEM. *Student's t test* was used in A, **P*<0.05, ***P*<0.01; n represents separate experiments, n=3. (**B**) Compared with that of control mice (**a, b, a′, b′, a″, b″, i, j, i′, j′, q, r, q′, r′**), the expression of Lhx5 was reduced in double-mutant mice at E11.5 (**c, d, c′, d′, c″, d″**), E13.5 (**k, l, k′, l′**), and E14.5 (**s, t, s′, t′**); the expression of Lhx2 was

Figure 5 continued on next page

Figure 5 continued

comparable between the control and double-mutant mice at E11.5 (**e–h, e′–h′**); and compared with that of control mice (**m, n, m′, n′, u, v, u′, v′**), the expression of Lhx2 was increased in double-mutant mice at E13.5 (**o, p, o′, p′**) and E14.5 (**w, x, w′, x′**). (**C**) Compared with that of control mice (**a, b, a′, b′**), the expression of Sox2 was normal in double-mutant mice at E14.5 (**c, d, c′, d′**); compared with that of control mice (**e, f, e′, f′**), the expression of Tbr2 was decreased in *Nr2f* mutant mice at E14.5 (**g, h, g′, h′**); compared with that of control mice (**i, j, i′, j′**), the expression of NeuroD1 was reduced in double-mutant mice at E14.5 (**k, l, k′, l′**). (**D**) Quantitative analysis of Tbr2-positive cells and NeuroD1-positive cells in (**Ce′–h′**) and (**Ci′–l′**). Data are presented as mean ± SEM. *Student's t test* was used in D, $^{**}P<0.01$; n represents separate experiments, n=3. (**E**), In the hippocampal primordium of the early embryo, *Nr2f1* is expressed dorsally in the MP, and *Nr2f2* is expressed ventrally in the CH. In the mature hippocampus, the expression of *Nr2f1* is higher in the dorsal hippocampus, which is related to spatial learning and memory, and the expression of *Nr2f2* is mainly in the ventral hippocampus, which is associated with emotion and anxiety (**a**). Our findings support a novel molecular mechanism by which *Nr2f1* and *Nr2f2* may cooperate to ensure the appropriate morphogenesis and functions of the hippocampus by modulating the *Lhx5-Lhx2* axis (**b**). CH, cortical hem; ChP, choroid plexus; DP, dorsal pallium; HP, hippocampal primordium; MP, medial pallium. Scale bars, (**Ba–x, Ca–l**), 200 μm; (**Ba′-x′, Ba″-d″, Ca′-l′**), 100 μm.

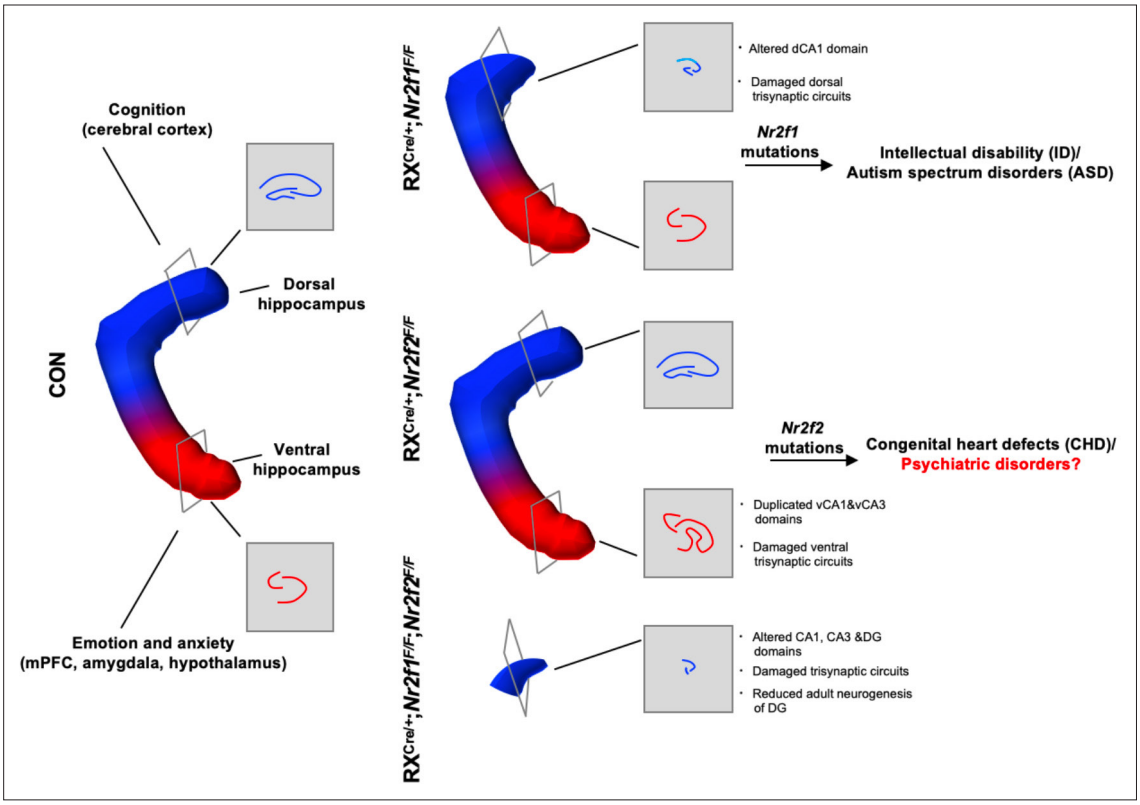

Figure 5—figure supplement 1. *Nr2f1* and *Nr2f2* genes coordinate to control distinct characteristics of the hippocampus. Roles of *Nr2f1* and *Nr2f2* genes in the development and function of the hippocampus and the association with neurological diseases. *Nr2f1* is required for the morphogenesis of the dorsal hippocampus and the specification of dorsal CA1 pyramidal neuron lineage, which are associated with neurodevelopmental disorders, including intellectual disability (ID) and autism spectrum disorders (ASD). *Nr2f2* is required to prevent the duplication of the CA1 and CA3 lineages of the ventral hippocampus, which may be related to psychiatric diseases such as depression, anxiety, or schizophrenia. The *Nr2f1* and *Nr2f2* genes are novel intrinsic regulatory genes, which cooperate with each other to ensure the early morphogenesis of the hippocampus.